Polymer Degradation and Stability 129 (2016) 133–141

Contents lists available at ScienceDirect

Polymer Degradation and Stability

journal homepage: www.elsevier.com/locate/polydegstab

Phosphorus-nitrogen containing polymer wrapped carbon nanotubes and their flame-retardant effect on epoxy resin

Shijun Wang [a], Fei Xin [a, *], Yu Chen [b], Lijun Qian [a], Yajun Chen [a]

[a] Department of Materials Science & Engineering, Beijing Technology and Business University, Beijing 100048, PR China
[b] Beijing Huateng Hightech Co.,Ltd., Beijing 100048, PR China

ARTICLE INFO

Article history:
Received 22 January 2016
Received in revised form
23 March 2016
Accepted 10 April 2016
Available online 20 April 2016

Keywords:
Carbon nanotubes
Flame retardant
Epoxy resin

ABSTRACT

A novel phosphorus-nitrogen containing polymer wrapped carbon nanotubes (CNT-PD-x, x denoted the feed ratio) were facilely prepared via strong π-π stacking interactions between the poly(-phenylphosphonic-4,4'-diaminodiphenyl-methane) (PD) and the walls of carbon nanotubes (CNTs). The content of polymer PD of CNT-PD-x can be controlled by adjusting the feed ratio of polymer monomers to CNTs. The structure and properties of CNT-PD-x were characterized by Fourier transformed infrared (FT-IR) spectroscopy, ^{1}H nuclear magnetic resonance (^{1}H NMR), transmission electron microscopy (TEM) and thermo gravimetric analysis (TGA) measurements. The CNT-PD-x was incorporated into epoxy resin for improving the flame retardancy. The LOI value reached to 33.6% when the mass fraction of CNT-PD-x (x = 20) was 4 wt%. Compared with CNTs, the same addition of CNT-PD-x (x = 10) reduced the PHRR and THR of epoxy resin more effectively. The results implied the gas-condensed phase flame-retardant effect of CNT-PD-x, which is ascribed to the combined action of the polymer PD and CNTs on the flame retardancy of epoxy resin.

1. Introduction

Epoxy resins (EP) have been industrialized for about 60 years and are widely used in various practical applications, especially as structural adhesive, protective coating and electrical encapsulation material due to their remarkable adhesion to many substrates, low shrinkage on cure, excellent mechanical properties and corrosion resistance [1–5]. However, epoxy resins have low flame retardancy that limits their high-performance applications for safety consideration [6]. Thus, it is important to improve the flame retardancy of epoxy resins. Currently, research on flame-retardant epoxy resins have focused on three ways, direct incorporating flame-retardant additives [7,8], building inherent flame-retardant epoxy resin molecules [9,10] and building flame-retardant curing agents of epoxy resin [11,12].

To obtain a highly efficient flame-retardant epoxy resin, the syntheses of some phosphorus-nitrogen containing flame retardants have already been conducted, such as hexa-(phospha-phenanthrene-hydroxyl-methyl-phenoxyl)-cyclotriphosphazene (HAP-DOPO) [13,14], tri-(3-DOPO-2-hydroxypropan-1-yl)-1,3,5-triazine-2,4,6-trione (TGIC-DOPO) [15,16], poly(melamine-ethoxyphosphinyl-diisocyanate) (PMPC) [17] and 1,3,5-tris(2-DOPO-10-ethyl)1,3,5-triazine-2,4,6(1H,3H,5H)-trione (DOP-Cy) [18]. Moreover, carbon nanotubes (CNTs) have drawn intensive interest and are considered to be a promising candidate for improving the flame retardancy of polymer in recent decades [19–22]. The improvement of flame retardancy is attributed to the formation of network char layer created by decomposition of CNTs which can hinder the heat and mass transport [23,24]. However, the flame retardancy efficiency of the CNTs is closely related to its dispersion in the polymeric matrix [25]. Much effort has been devoted to improve the dispersibility of the CNTs through covalent and non-covalent functionalization. For instance, Fang et al. prepared intumescent flame retardant covalently grafted CNTs, which showed better dispersion and flame-retardant effect [26,27]. Molybdenum-phenolic resin was grafted onto the surface of CNTs, which improved the dispersion of CNTs in epoxy resin and showed high char yield during combustion [28]. CNTs wrapped with MoS_2 nanolayers were well-dispersed in the EP matrix, leading to simultaneous improvement of flame retardancy and mechanical properties [29]. Although many functionalized methods have been reported, the high-performance CNTs are still necessary to be

* Corresponding author. Gengyun Building No.9906, Fucheng Road No.11, Haidian District, Beijing, PR China. Tel.: +86 10 68985531.
E-mail address: xinfei@th.btbu.edu.cn (F. Xin).

http://dx.doi.org/10.1016/j.polymdegradstab.2016.04.011
0141-3910/

further explored at low loading.

In this work, a novel phosphorus-nitrogen containing polymer, poly(phenylphosphonic-4,4'-diaminodiphenyl-methane) (PD) was wrapped on the surface of CNTs by strong π-π stacking interactions to obtain CNT-PD-x. The wrapped CNTs were mixed into diglycidyl ether of bisphenol-A (DGEBA) to prepare non-halogen flame-retardant epoxy resins. The flame-retardant behaviors of epoxy resins containing CNT-PD-x were systematically characterized and the flame-retardant effects of CNT-PD-x were also analyzed.

2. Experimental

2.1. Materials

Multi-walled CNTs with a diameter of less than 8 nm were purchased from Chengdu Institute of Organic Chemistry, China. Phenylphosphonic dichloride (PPD), 4,4′-Diaminodiphenyl methane (DDM) and triethylamine (TEA) were supplied by Sinopharm Chemical Reagent Co. Ltd., China. Tetrahydrofuran (THF) was purchased from Beijing Chemical reagent Co. Ltd., China. The epoxy resin, diglycidyl ether of bisphenol-A (DGEBA, commercial name: E-51), was purchased from Blue Star New Chemical Material Co. Ltd., China.

2.2. Preparation of CNT-PD-x and PD

The wrapped CNTs, designated as CNT-PD-x (x = 5, 10 and 20, x denoted the feed ratio of polymer monomers to CNTs) with various contents of polymer PD of CNT-PD-x (C_{PD}), were prepared as follows. 1.00 g of CNTs, excess TEA as acid acceptor and 200 mL THF were fed into a 500-mL three-necked flask and placed in an ultrasonic bath (300 W, 80 kHz) for 30 min. Then the mixture was stirred and cooled to 5 °C in an ice-water bath. Subsequently, a certain amount of PPD was added into the above mixture. After the PPD was mixed uniformly, a THF solution of DDM was added dropwise to the mixture for 1 h with vigorous stirring while keeping the reaction system cool. Then the reaction mixture was maintained at 50 °C for 12 h at reflux. Finally, the reaction mixture was filtered to remove the solvent, and the product was washed with THF three times and then with deionized water at least three times. The resulting product was dried in a vacuum at 80 °C for 12 h to a constant weight. Moreover, in order to determine the C_{PD}, a phosphorus-nitrogen containing polymer PD was synthesized using the same method without the addition of CNTs. The synthesis procedure is shown in Scheme 1, and the experimental formulae are given in Table 1.

2.3. Preparation of flame-retardant epoxy resins

The CNT-PD-x powder was added into EP under mechanical stirring at room temperature. Then the mixture was heated slowly to 110 °C and stirred until CNT-PD-x was evenly dispersed in EP. After the mixture was cooled to 100 °C, DDM as curing agent was added and dissolved completely to form a uniform mixture. The mixture was kept in a vacuum oven at 100 °C for 3 min for degassing. Then the mixture was poured into the preheated molds and cured at 120 °C for 2 h and then at 170 °C for 4 h. Moreover, the 2%PD/EP and 4%PD/EP samples with polymer PD instead of CNT-PD-x were prepared with the same method. The 2%CNT/EP and 4%CNT/EP samples with CNTs instead of CNT-PD-x were also prepared with the same method. The Pure EP sample was also made in the same method without the addition of flame retardant.

All the details of formulae are listed in Table 2.

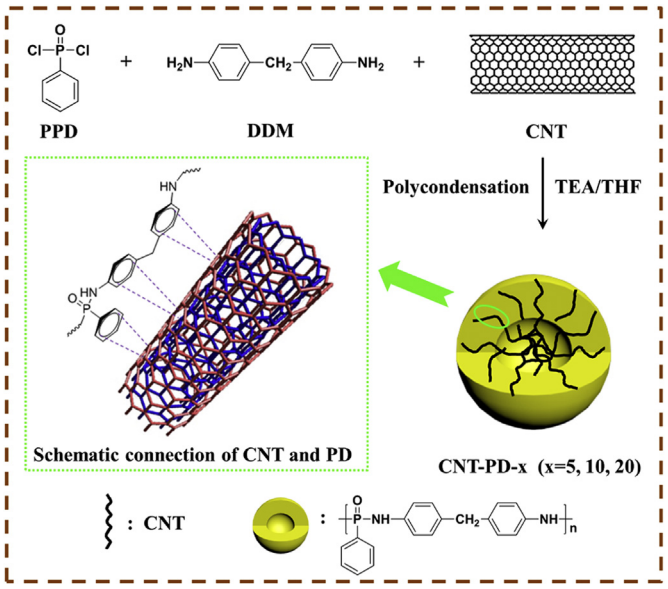

Scheme 1. Schematic illustration of the synthesis procedure of CNT-PD-x.

Table 1
The experimental formulae and information on CNT-PD-x.

CNT-PD-x	CNT (g)	TEA (g)	PPD (g)	DDM[a] (g)	Yield (%)	C_{PD} (wt.%)
CNT-PD-5	1.00	3.09	2.48	3.02	60.3	77.1
CNT-PD-10	1.00	6.18	4.96	6.05	70.6	80.8
CNT-PD-20	1.00	12.36	9.92	12.10	75.6	92.7

[a] The amounts of DDM used were 120 wt% of the theoretical amount required.

Table 2
The formulae of the epoxy resin thermosets.

Samples	EP (g)	DDM (g)	CNTs or CNT-PD-x (x = 5, 10, 20)	
			(g)	(wt.%)
Pure EP	100	25.3	0	0
2%CNT/EP	100	25.3	2.6	2
4%CNT/EP	100	25.3	5.2	4
2%PD/EP	100	25.3	2.6	2
4%PD/EP	100	25.3	5.2	4
2%CNT-PD-5/EP	100	25.3	2.6	2
4%CNT-PD-5/EP	100	25.3	5.2	4
2%CNT-PD-10/EP	100	25.3	2.6	2
4%CNT-PD-10/EP	100	25.3	5.2	4
2%CNT-PD-20/EP	100	25.3	2.6	2
4%CNT-PD-20/EP	100	25.3	5.2	4

2.4. Characterizations

The Fourier transform infrared (FTIR) spectra were obtained on a Nicolet iN10MX type spectrometer. The powdered samples were thoroughly mixed with KBr and then pressed into pellets.

Hydrogen^{-1} nuclear magnetic resonance (^{1}H NMR) was obtained using a Bruker AV300MB NMR spectrometer and a DMSO-d_6 solvent.

Morphology of CNTs and CNT-PD-x were observed with a JEM 2100 transmission electron microscope (TEM) at an accelerating voltage of 100 kV.

Thermo gravimetric analysis (TGA) was recorded on TA instrument Q500 IR thermal gravimetric analyzer with a heating rate of 20 °C/min from 40 to 600 °C under N_2 atmosphere. All the tests

were repeated three times, and the typical TGA data were reproducible within ±5%.

The limiting oxygen index (LOI) values were obtained on a FTT (Fire Testing Technology, UK) Dynisco LOI instrument according to ASTM D 2863-97 (sample size: 130 mm × 6.5 mm × 3.2 mm).

The fire behavior was characterized on a FTT cone calorimeter according to ISO5660 under an external heat flux of 50 kW/m^2 (sample size: 100 mm × 100 mm × 3 mm). The measurement for each specimen was repeated three times, and the error values of the typical cone calorimeter data were reproducible within ±5%.

The dispersion of CNTs and CNT-PD-x were examined using a FP 2032/14 Quanta 250 FEG scanning electron microscope (SEM) under high vacuum with a voltage of 10 kV. The micromorphology of the residual char from the cone calorimeter test was obtained using scanning electron microscope (SEM, Tescan Vega II, Tescan SRO Co., Czech Republic) under high vacuum with voltage of 20 kV. The SEM instrument was fully integrated with an energy dispersive X-ray (EDX) microanalyser for elemental analysis.

To recognize the pyrolysis fragments of polymer PD, a Shimadzu GC-MS-QP5050A gas chromatography-mass spectrometer equipped with a PYR-4A pyrolyzer was employed. The helium (He) was utilized as carrier gas for the volatile products. The injector temperature was 250 °C, the temperature of GC/MS interface was 280 °C and the cracker temperature was 500 °C.

3. Results and discussion

3.1. Characterization of CNT-PD-x

Fig. 1 shows the FTIR spectra of CNTs, PD and CNT-PD-10. For CNTs, they have few identifiable functional groups. The peak at 1579 cm^{-1} is attributed to an in-plane E_{1u} mode of monocrystalline graphite [28]. In the FTIR spectra of PD, it is observed that the strong absorption peaks at 1510 and 1613 cm^{-1} are attributed to the vibration of the benzene ring skeleton. The broad absorption peak at around 3422 cm^{-1} is attributed to the stretching vibration of N—H. The characteristic peaks centered at 1288 and 1438 cm^{-1} correspond to P═O and P-Ph, respectively. The absorption peak at 1122 cm^{-1} indicates the formation of the P—N. Meanwhile, the absorption peak at 550 cm^{-1} corresponding to the P—Cl bond disappear. Therefore, it can be deduced that the PPD was reacted with the DDM and the phosphorus-nitrogen containing polymer PD was successfully synthesized. Furthermore, these characteristic peaks in the spectrum of PD also appear in the spectrum of CNT-PD-10. It shows that the polymer PD exists in CNT-PD-10.

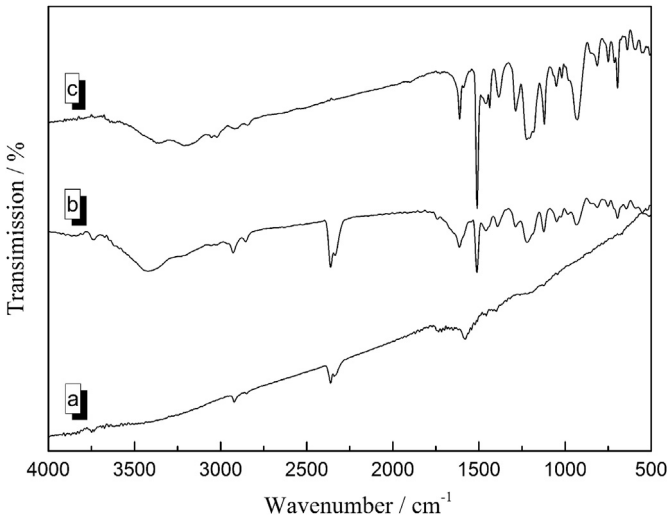

Fig. 1. The FTIR spectra of (a) CNTs, (b) PD and (c) CNT-PD-10.

The ^{1}H NMR spectrum was further used to investigate the structural of PD. As shown in Fig. 2, the peaks of ^{1}H NMR (DMSO-d_6, ppm): $\delta = 7.3$ to 8.0 (benzene ring, 4H), $\delta = 6.7$ to 7.1 (benzene ring, 5H), $\delta = 3.0$ to 3.1 (N—H, 1H), $\delta = 1.1$ to 1.3 (—CH_2, 2H) were found in ^{1}H NMR of PD. The results of FTIR and ^{1}H NMR clearly indicated that CNT-PD-10 has been successfully prepared.

In order to get the morphology of evidence, the comparison for TEM images of CNTs and CNT-PD-10 are presented in Fig. 3. Fig. 3(a) displays a typical TEM image of CNTs, showing very smooth surface and clear tubes. From the TEM image of CNT-PD-10 in Fig. 3(b), the surface of CNTs became obscure and roughness because the polymer PD wrapped on the external surface of CNTs. In addition, the increase of diameters of CNTs is discerned from CNT-PD-10 in Fig. 3 (b). The polymer PD is tightly wrapped on the surface of CNTs, because there is a strong π-π stacking interaction between the polymer PD and the walls of CNTs. Undoubtedly, the TEM images provide a further direct evidence of the wrapping of CNT-PD-10.

Fig. 4 shows the TGA curves of CNTs, PD, and CNT-PD-x, which were carried out from 40 °C to 600 °C at 20 °C/min under N_2 atmosphere. Obviously, CNTs presented good thermal stability under N_2 atmosphere. When the temperature was increased up to 600 °C, there was no evident decomposition in CNTs, with 96.2 wt% of residue at that temperature. The synthesized phosphorus-nitrogen containing polymer PD started to decompose at 258 °C and about 33.0 wt% of residue was left at 600 °C, indicating PD has a good char-forming capability. For CNT-PD-5, CNT-PD-10 and CNT-PD-20, about 47.5 wt%, 45.1 wt% and 37.6 wt% of residues were left at 600 °C, respectively. By comparing the differences in the weight loss between CNTs, PD, and CNT-PD-x, the content of the polymer PD in CNT-PD-x was roughly estimated using the following equation:

$$W_{CNT-PD-x} = (1 - C_{PD}) \times W_{CNTs} + C_{PD} \times W_{PD} \quad (1)$$

where W_{CNTs}, W_{PD}, and $W_{CNT-PD-x}$ were the residues weight fractions of CNTs, PD, and CNT-PD-x at 600 °C, respectively. C_{PD} denoted the content of the polymer PD in CNT-PD-x.

Considering that the mutual influence on thermal degradation between PD and CNTs is possible, thus the C_{PD} is only approximate but not accurate. The calculated C_{PD} is listed in Table 1. As expected, the C_{PD} increases with the increase of the feed ratio of polymer monomers to CNTs.

3.2. Dispersion of CNTs and CNT-PD-x in the thermosets

The reinforcement potential of CNTs is remarkably dependent on the dispersion of CNTs in the thermosets. Therefore, it is necessary to determine the dispersibility of CNTs in the thermosets. The dispersion of CNTs and CNT-PD-x were examined by SEM, as shown in Fig. 5. The fracture surface of Pure EP in Fig. 5(a) was smooth without nanofillers. In Fig. 5(b), it was observed that CNTs agglomerated seriously in the thermosets due to the van der Waals force between CNTs. In contrast, CNT-PD-10 showed a good dispersion in the thermosets and no obvious aggregation was observed in Fig. 5(c). This indicates that the polymer PD wrapped on the surface of CNTs preventing the agglomeration of CNTs and improving the dispersion of CNTs in the thermosets.

3.3. LOI test

The LOI values of all samples were measured, and the corresponding results are presented in Fig. 6. It can be seen that the presence of CNTs increased the LOI value of EP only slightly. When

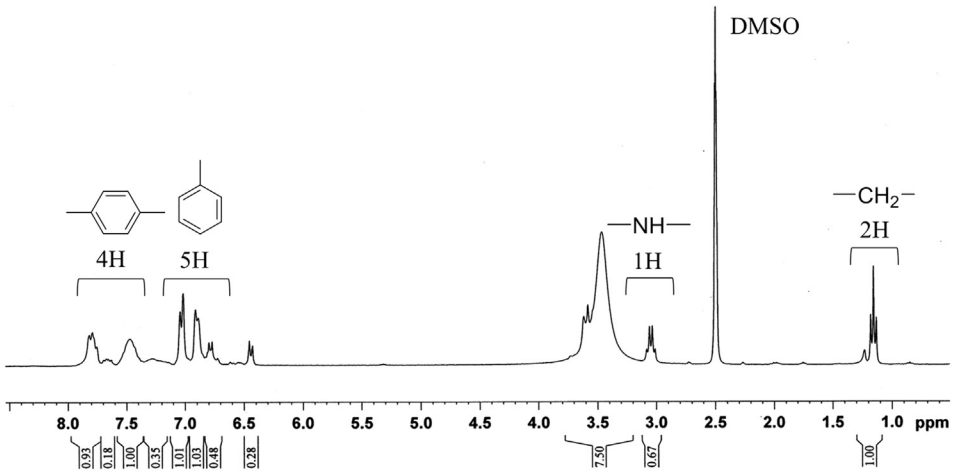

Fig. 2. The ^{1}H NMR spectrum of PD.

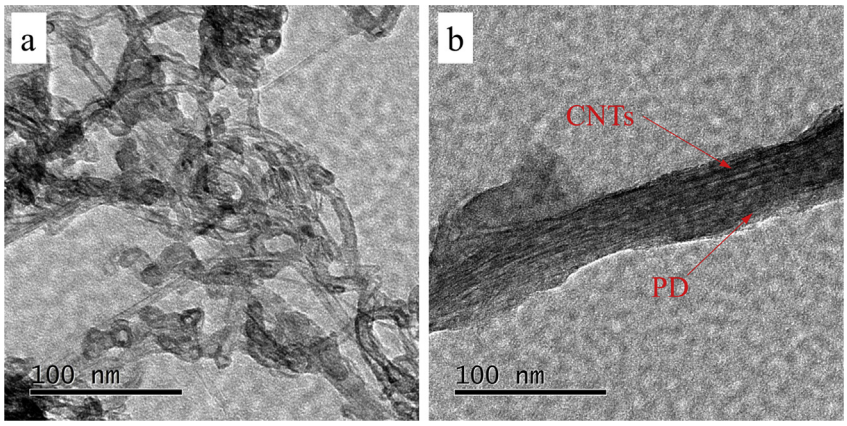

Fig. 3. TEM images of (a) CNTs and (b) CNT-PD-10.

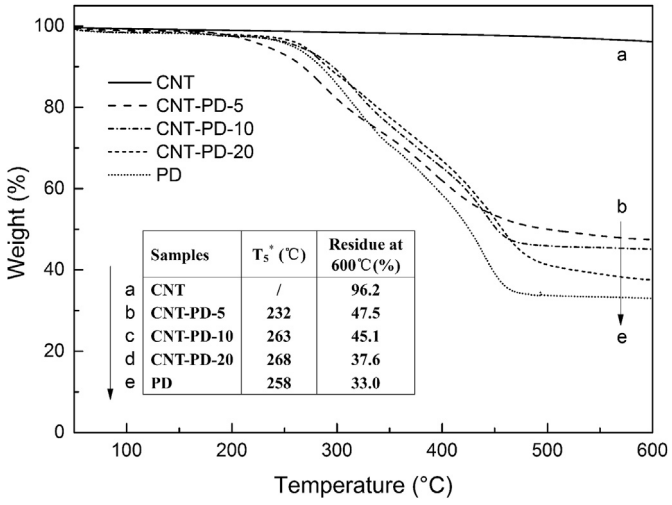

Fig. 4. TGA curves of (a) CNTs, (b) CNT-PD-5, (c) CNT-PD-10, (d) CNT-PD-20 and (e) PD. *T_5 = the temperature at which 5 wt% weight loss takes place.

the mass fractions of CNTs were 2 wt% and 4 wt%, the LOI values of CNT/EP only increased from 26.3% to 26.8% and 27.3%, respectively. It shows that CNTs merely exhibited flame retardancy at a low level to EP thermosets. However, the wrapped CNTs significantly improved the LOI values of EP thermosets, the LOI value of CNT-PD-20/EP increased to 33.6% when the mass fraction of CNT-PD-20 was only 4 wt%. The LOI values of CNT-PD-x/EP (x = 5, 10, 20) samples were also higher than those of PD/EP samples (2%PD/EP: 29.6%, 4% PD/EP: 30.9%), this was due to the combined action of PD and CNTs on the flame retardancy of epoxy resin. After comparing the LOI values of the same addition of 2%CNT-PD-x/EP (x = 5, 10, 20) samples, the LOI values firstly increased and then decreased with the increasing feed ratio. The result can be related with the weight ratio of polymer PD to CNTs in the EP thermoset and the suitable C_{PD} should be possessed a better flame-retardant effect. Moreover, in the same C_{PD}, the LOI values of EP thermosets also increased with the increasing of wrapped CNTs addition. In a word, the flame retardancy of wrapped CNTs is obviously superior to that of CNTs. The deduction will be further discussed in the subsequent section.

3.4. Cone calorimeter test

Cone calorimeter test is a fire testing apparatus based on the oxygen consumption principle and provides a wealth of information on flammability characteristics of materials [30,31]. The partial characteristic parameters of samples, such as peak of heat release rate (PHRR), total heat release (THR), average effective combustion heat (av-EHC), average yield of CO (av-COY), average yield of CO_2 (av-CO_2Y) and the char yield, are shown in Table 3 and Figs. 7 and 8.

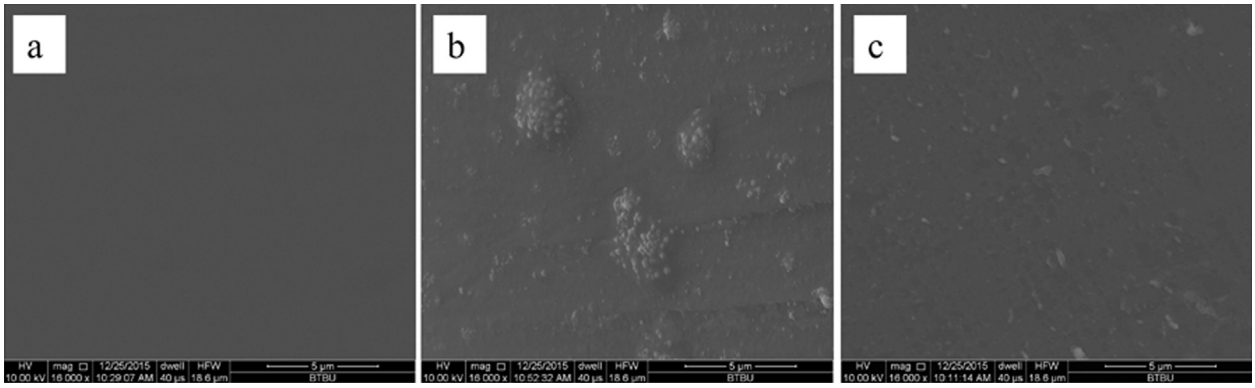

Fig. 5. SEM images of fracture surfaces of (a) Pure EP, (b) 2%CNT/EP and (c) 2%CNT-PD-10/EP.

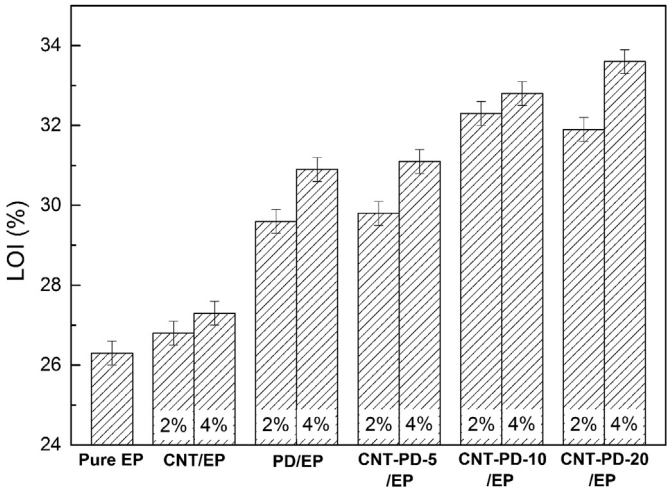

Fig. 6. The LOI values of the epoxy resin thermosets.

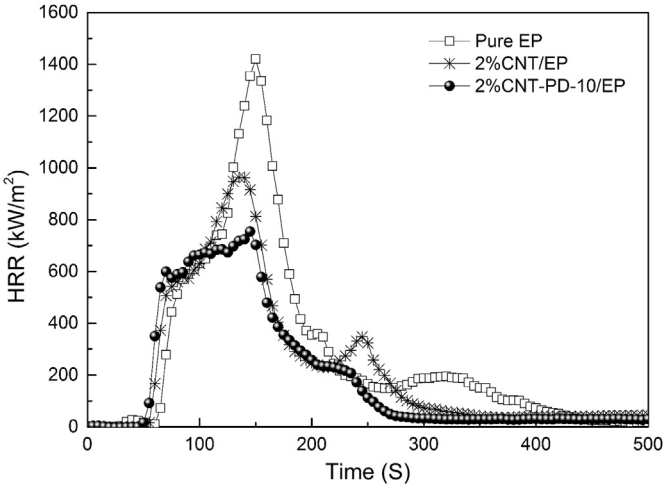

Fig. 7. The HRR curves of Pure EP, 2%CNT/EP and 2%CNT-PD-10/EP.

Table 3
The parameters of samples investigated by the cone calorimeter test.

Samples	PHRR (kW/m^2)	THR (MJ/m^2)	av-EHC (MJ/kg)	av-COY (kg/kg)	av-CO_2Y (kg/kg)	Char yield (%)
Pure EP	1420 ± 53	144 ± 5	29.9 ± 0.3	0.126 ± 0.005	2.51 ± 0.10	8.81 ± 0.25
2%CNT/EP	963 ± 36	119 ± 3	26.4 ± 0.3	0.101 ± 0.004	2.16 ± 0.09	9.75 ± 0.27
2%CNT-PD-10/EP	754 ± 31	102 ± 3	23.6 ± 0.2	0.132 ± 0.005	1.90 ± 0.08	14.70 ± 0.32

As shown in Fig. 7, the HRR curves of Pure EP and 2%CNT/EP had a small shoulder after ignition and before PHRR. This characteristic curve of HRR represents non-charring materials [32]. At the end of combustion, the Pure EP and 2%CNT/EP formed only small amounts of residue, which hardly influenced the shape of the HRR curve. The HRR curve of 2%CNT-PD-10/EP showed a gentle rise after strong initial increase up to the occurring of PHRR. This was due to the 2% CNT-PD-10/EP formed a thicker intumescent char, which showed effective barrier effect. Fig. 8 shows the mass loss curves of the Pure EP, 2%CNT/EP and 2%CNT-PD-10/EP. The mass loss curve characterizes the reduction of mass of the material during combustion. At the end of combustion (500s), the char yield of 2%CNT-PD-10/EP was obviously more than those of Pure EP and 2%CNT/EP. Therefore, the wrapped CNTs present better charring than CNTs.

The quantitative assessment of flame retardancy can precisely compare the difference between CNTs and CNT-PD-x in flame-retardant effect. The gas-phase effect and charring are quantified by the reduction of the effective heat of combustion of the volatiles (av-EHC) and the increase in residue, respectively. The change of THR is attributed to the changes of the effective heat of combustion and the amount of released fuel, and the change of PHRR is attributed to the changes of the effective heat of combustion, the amount of released fuel and the barrier effect of the char [33,34]. In Table 3, the av-EHC of 2%CNT/EP was reduced to 88.3% compared with that of the Pure EP. The residue increased from 8.81% to 9.75%, thus the amount of released fuel was reduced to 99.0% [(1–9.75%)/(1–8.81%)]. The change of THR is correspond to the lowered effective heat of combustion and decreased fuel available (88.3% × 99.0% = 87.4%, the tested value is 83.1%). The PHRR was reduced to 67.8%. Hypothetically, a reduction of the PHRR to 87.4% is attributed to the gas-phase effect and increased charring as discussed for the THR. The additional reduction of the PHRR comes from the barrier effect of the intumescent char. This relative value is then calculated to be 22.4% (1–67.8%/87.4%). This result demonstrates that the barrier effect plays a main role in the flame retardancy of 2%CNT/EP.

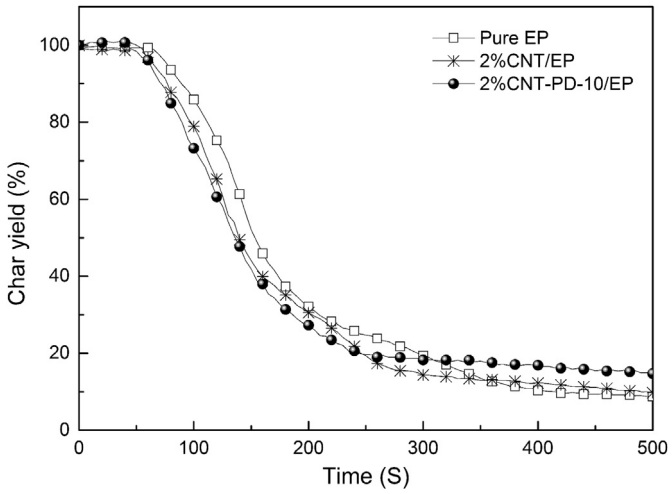

Fig. 8. Normalized mass loss curves of Pure EP, 2%CNT/EP and 2%CNT-PD-10/EP from the cone calorimeter test.

The method also can be used for calculation of 2%CNT-PD-10/EP. The av-EHC was reduced to 78.9% due to the gas-phase effect of CNT-PD-10. The residue increased to 14.70%, thus the amount of released fuel was reduced to 93.5% [(1−14.70%)/(1−8.81%)]. The reduction of THR is also attributed to the reductions of the effective heat of combustion and amount of fuel (78.9% × 93.5% = 73.8%, the tested value is 70.7%). The PHRR was reduced to 53.1%. A reduction to 73.8% is assumed to originate from the gas-phase effect and the increased residue of CNT-PD-10. The additional reduction of the PHRR also comes from the barrier effect of the intumescent char. This relative value is then calculated to be 28.1% (1−53.1%/73.8%). It shows that the barrier effect of the intumescent char is significant for 2%CNT-PD-10/EP.

Moreover, the differences of flame retardancy mechanisms of 2% CNT/EP and 2%CNT-PD-10/EP are further compared. In condensed phase, the charring and barrier effects of 2%CNT-PD-10/EP (6.5% and 28.1%) are stronger than those of 2%CNT/EP (1.0% and 22.4%), which just accords with the characteristics of char yield in Fig. 8. The reason is deduced that the interaction of the products from the pyrolysis of the phosphorus-nitrogen containing polymer PD and EP matrix promoted charring of the thermosets, and the interaction also enhanced the barrier effect of the char. Thus the reinforced intumescent char of 2%CNT-PD-10/EP is more effective to hinder the heat and mass transport compared with that of 2%CNT/EP. The further evidences in detail will be provided in the following discussion. Moreover, the gas-phase effect of 2%CNT-PD-10/EP (21.1%) is also stronger than that of 2%CNT/EP (11.7%). Combining with the data of Py-GC/MS in the later discussion, it is concluded that the fragments released during the pyrolysis of CNT-PD-10 presented quenching effect and restrained the ignition of combustible volatiles resulting in more incomplete combustion. Thus the CO/CO_2 ratio was increased from 5.01% to 6.94%. In the 2%CNT/EP, CNTs released CO_2 during combustion, which diluted combustible volatiles resulting in the reduction of the CO/CO_2 ratio to 4.68%, but this effect is very low.

3.5. Morphology analysis of residues from cone calorimeter test

The condensed-phase flame-retardant effects of the Pure EP, 2% CNT/EP and 2%CNT-PD-10/EP were further investigated using a digital camera and SEM with EDX. The macro-morphology images of the residues after the cone calorimeter test are shown in Fig. 9. As shown in Fig. 9(a), the residue from Pure EP sample reserved only tiny amounts of badly broken char, which means that Pure EP almost totally decomposed during combustion. The residue of 2% CNT/EP in Fig. 9(b) presented the local destruction, and the expansion ratio was not obvious. However, in Fig. 9(c), the residue of 2%CNT-PD-10/EP was compact and complete, a preferable intumescent char, which not only effectively hampered the heat and mass transfer but also increased the char yield.

In order to further explore the charring and barrier effects of 2% CNT-PD-10/EP, SEM images of cone calorimeter residues are shown in Fig. 10. From direct observations, the residue of Pure EP in Fig. 10(a) had a lot of open holes with different sizes, which provided channels for the combustible volatiles from the inner matrix and heat feedback from the flame. In Fig. 10(b), the residue of 2% CNT/EP appeared many cracks and fissures because the undispersed network char layer created by decomposition of CNTs was brittle and easy to be damaged. Obviously, the residue of 2%CNT-

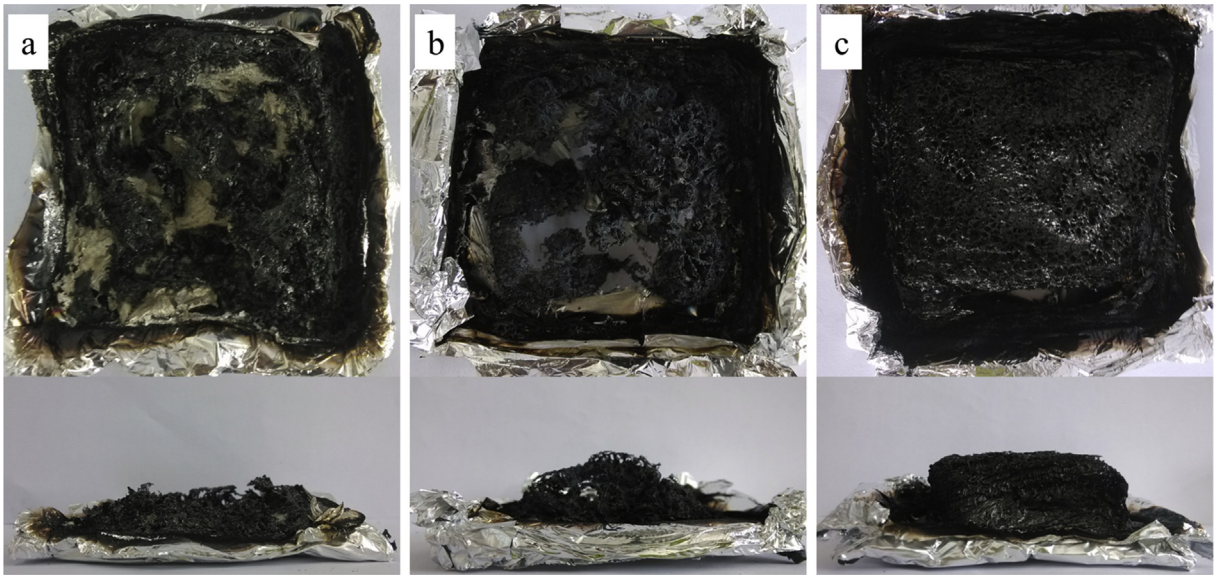

Fig. 9. Digital photos of cone calorimeter residues of (a) Pure EP, (b) 2%CNT/EP and (c) 2%CNT-PD-10/EP.

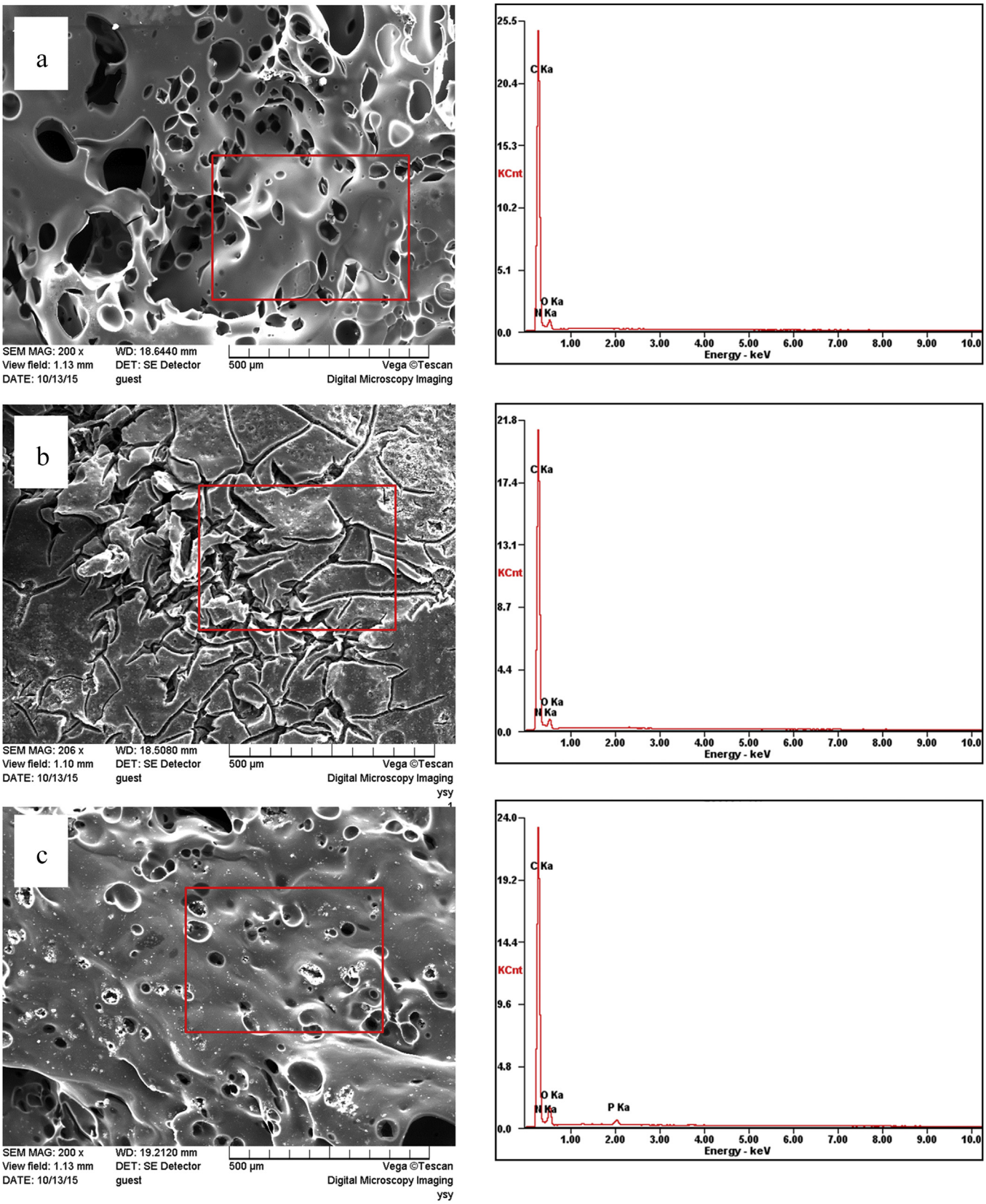

Fig. 10. SEM images and EDX analysis of cone calorimeter residues of (a) Pure EP, (b) 2%CNT/EP and (c) 2%CNT-PD-10/EP.

PD-10/EP in Fig. 10(c) was very dense, and few open holes were found. This can be explained by the facts that, on one hand, the wrapped CNTs formed a continuous network structured protective layer; on the other hand, the polymer PD in CNT-PD-10 generated

some products to fill the gap of the network char layer of CNTs to make it denser. Therefore, this residue structure can effectively seal the combustible volatiles in the matrix and decrease the combustion intensity.

Additionally, the elemental composition and content of cone calorimeter residues were determined using EDX. The EDX data are given in Fig. 10 and Table 4. In the case of 2%CNT-PD-10/EP, it is markedly found the occurrence of phosphorus and the increase of oxygen content on surface of residue. It confirms that the CNT-PD-10 decomposed to form some viscous polyphosphates and their related analogues in the condensed phase during combustion, which can enhance the barrier effect of the char layer. Thus the more significant condensed-phase flame retardancy was obtained.

Table 4
EDX data of surface of residues.

Samples	Element content (wt.%)			
	C	O	N	P
Pure EP	82.46	7.08	10.46	0
2%CNT/EP	82.21	7.89	9.90	0
2%CNT-PD-10/EP	78.21	11.98	9.14	0.67

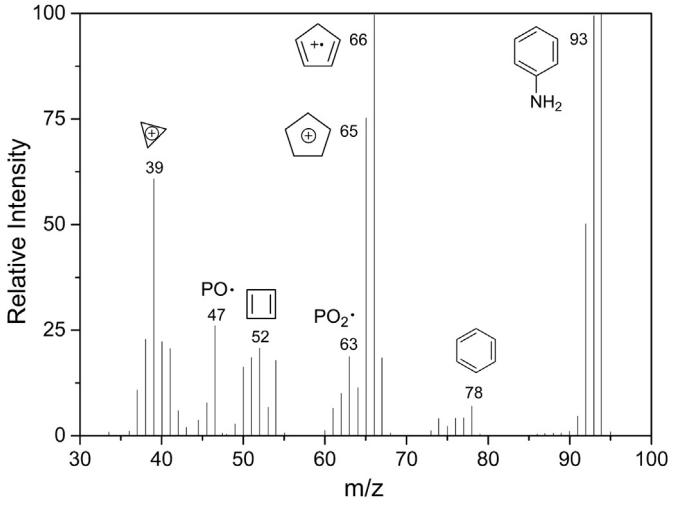

Fig. 11. Py-GC/MS spectrum of PD and the deduced chemical structure of typical *m/z* peaks.

3.6. Py-GC/MS analysis of PD

The pyrolysis behavior of polymer PD was disclosed to explain why CNT-PD-x exerts the gas-phase flame-retardant effect. PD was pyrolyzed at 500 °C and the characteristic fragments were detected by GC/MS. The typical fragment flows with some characteristic ionic peaks were selected, and the results are shown in Fig. 11. PD is the polycondensation product of PPD and DDM, which means that PD was firstly decomposed into some parts containing benzene ring: aniline ($m/z = 93$) and benzene ring ($m/z = 78$). Subsequently, the further pyrolysis of the parts containing benzene ring would generate a series of inert free radicals, such as C_5H_6 ($m/z = 66$), C_5H_5 ($m/z = 65$), C_4H_4 ($m/z = 52$) and C_3H_3 ($m/z = 39$). The fragment ionic peaks at m/z 63 and 47 were determined as PO_2• and PO• free radicals, respectively. These two free radicals can quench the active chain reaction free radicals from the decomposed matrix and reduce the effective heat of combustion of the volatiles, which has been reported by many papers concerned [15,35]. Therefore, CNT-PD-x exerts the quenching effect in gas phase, which also confirmed the above inference.

3.7. Flame-retardant mechanism of CNT-PD-x in EP thermosets

According to all the discussed results, the flame-retardant mechanism of CNT-PD-x in EP thermosets is illustrated in Fig. 12. After the flame-retardant EP thermosets are ignited, the pyrolysis of CNT-PD-x releases some fragments with quenching effect to the gas phase resulting in more incomplete combustion, and the fragments inhibit the intensity of flame, which exhibits a gas-phase flame-retardant mechanism. In the condensed phase, on one hand, the CNTs in CNT-PD-x forms a continuous network char layer; on the other hand, the phosphorus-nitrogen containing polymer PD produces some viscous polyphosphates and their related analogues with strong dehydration property, which not only fill the gap of the network char layer of CNTs but also promote the charring of EP matrix. Therefore, the presence of CNT-PD-x is conducive to EP thermosets form markedly intumescent char, which can prohibit the release of combustible volatiles from the inner matrix and heat feedback from the flame. In a word, the CNT-PD-x has a gas-condensed phase flame-retardant effect in which the barrier effect of the intumescent char plays a main role.

4. Conclusion

A novel phosphorus-nitrogen containing polymer wrapped CNTs, CNT-PD-x, were facilely prepared via strong π-π stacking interactions between the polymer PD and the walls of CNTs. The C_{PD}

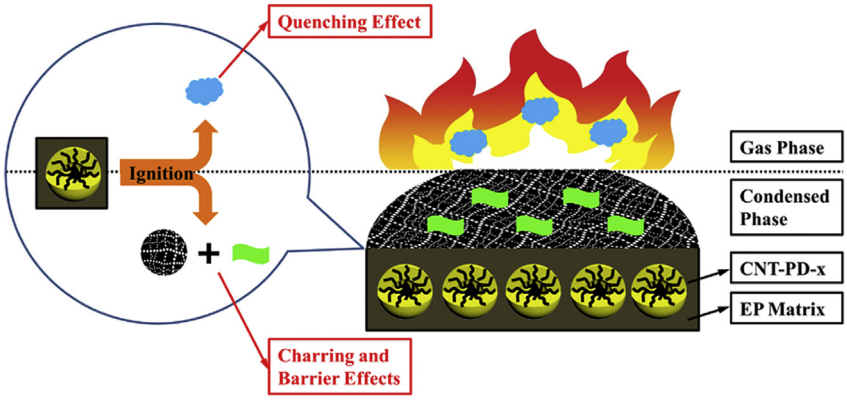

Fig. 12. The gas-condensed phase flame-retardant mechanism of CNT-PD-x.

of CNT-PD-x can be readily controlled by adjusting the feed ratio of polymer monomers to CNTs. The composition and morphology of CNT-PD-x exhibited that the polymer PD was wrapped on the surface of CNTs by non-covalent modification. CNT-PD-x showed outstanding flame-retardant effect on EP matrix compared with CNTs. This observation was confirmed by the results of the LOI and cone calorimeter tests. The LOI value of EP composite reached to 33.6% when the mass fraction of CNT-PD-20 was 4 wt%. The PHRR and THR values remarkably reduced by 46.9% and 29.3%, respectively, when the mass fraction of CNT-PD-10 was only 2 wt%. The results imply the gas-condensed phase flame-retardant effect of CNT-PD-x, which is ascribed to the combined action of the CNTs and the polymer PD on the flame retardancy of EP thermosets. In gas phase, the pyrolysis of CNT-PD-x can release some fragments with quenching effect, which reduced the effective heat of combustion of the volatiles. In condensed phase, the CNTs can form a continuous network char layer, and the polymer PD produces some viscous polyphosphates and their related analogues at the same time, which can cover the surface of network char layer and promote the charring of EP matrix. Therefore, CNT-PD-x imposes better flame retardancy to EP thermosets in gas-condensed phase than CNTs.

Acknowledgments

The work was supported by the National Nature Science Foundation of China (No.51403007), Supported by Beijing Excellent Talent Training Program (2013D005003000013) and Open fund project of Guangdong Province Enterprise Key Laboratory of Materials and Elements Fire Testing Technology (20130005).

References

[1] N. Chikhi, S. Fellahi, M. Bakar, Modification of epoxy resin using reactive liquid (ATBN) rubber, Eur. Polym. J. 38 (2) (2002) 251–264.
[2] R. Tripathy, U. Ojha, R. Faust, Polyisobutylene modified bisphenol A diglycidyl ether based epoxy resins possessing improved mechanical properties, Macromolecules 44 (17) (2011) 6800–6809.
[3] E.D. Weil, S. Levchik, A review of current flame retardant systems for epoxy resins, J. Fire Sci. 22 (1) (2004) 25–40.
[4] X. Wang, Y. Hu, L. Song, W.Y. Xing, H.D. Lu, P. Lv, G.X. Jie, Flame retardancy and thermal degradation mechanism of epoxy resin composites based on a DOPO substituted organophosphorus oligomer, Polymer 51 (2010) 2435–2445.
[5] B. Perret, B. Schartel, K. Stöß, M. Ciesielski, J. Diederichs, M. Döring, J. Krämer, V. Altstädt, Novel DOPO-based flame retardants in high-performance carbon fibre epoxy composites for aviation, Eur. Polym. J. 47 (2011) 1081–1089.
[6] L.J. Qian, Y. Qiu, J. Liu, F. Xin, Y.J. Chen, The flame retardant group-synergistic-effect of a phosphaphenanthrene and triazine double-group compound in epoxy resin, J. Appl. Polym. Sci. 131 (3) (2014) 39709.
[7] R.M. Perez, J.K.W. Sandler, V. Altstädt, T. Hoffmann, D. Pospiech, M. Ciesielski, M. Döring, U. Braun, A.I. Balabanovich, B. Schartel, Novel phosphorus-modified polysulfone as a combined flame retardant and toughness modifier for epoxy resins, Polymer 48 (3) (2007) 778–790.
[8] J.S. Wang, Y. Liu, H.B. Zhao, J. Liu, D.Y. Wang, Y.P. Song, Y.Z. Wang, Metal compound-enhanced flame retardancy of intumescent epoxy resins containing ammonium polyphosphate, Polym. Degrad. Stabil. 94 (2009) 625–631.
[9] C.L. Bao, Y.Q. Guo, L. Song, Y.C. Kan, X.D. Qian, Y.T. Hu, In situ preparation of functionalized graphene oxide/epoxy nanocomposites with effective reinforcements, J. Mater Chem. 21 (2011) 13290–13298.
[10] L.P. Gao, D.Y. Wang, Y.Z. Wang, J.S. Wang, B. Yang, A flame-retardant epoxy resin based on a reactive phosphorus-containing monomer of DODPP and its thermal and flame-retardant properties, Polym. Degrad. Stabil. 93 (7) (2008) 1308–1315.
[11] B. Schartel, U. Braun, A.I. Balabanovich, J. Artner, M. Ciesielski, M. Döring, R.M. Perez, J.K.W. Sandler, V. Altstädt, Pyrolysis and fire behaviour of epoxy systems containing a novel 9,10-dihydro-9-oxa-10-phosphaphenanthrene-10-oxide-(DOPO)- based diamino hardener, Eur. Polym. J. 44 (2008) 704–715.
[12] S. Levchik, A. Piotrowski, E. Weil, Q. Yao, New developments in flame retardancy of epoxy resins, Polym. Degrad. Stabil. 88 (3) (2005) 57–62.
[13] L.J. Qian, L.J. Ye, G.Z. Xu, J. Liu, J.Q. Guo, The non-halogen flame retardant epoxy resin based on a novel compound with phosphaphenanthrene and cyclotriphosphazene double functional groups, Polym. Degrad. Stabil. 96 (6) (2011) 1118–1124.
[14] L.J. Qian, L.J. Ye, Y. Qiu, S.R. Qu, Thermal degradation behavior of the compound containing phosphaphenanthrene and phosphazene groups and its flame retardant mechanism on epoxy resin, Polymer 52 (24) (2011) 5486–5493.
[15] L.J. Qian, Y. Qiu, N. Sun, M.L. Xu, G.Z. Xu, F. Xin, Y.J. Chen, Pyrolysis route of a novel flame retardant constructed by phosphaphenanthrene and triazine-trione groups and its flame-retardant effect on epoxy resin, Polym. Degrad. Stabil. 107 (2014) 98–105.
[16] L.J. Qian, Y. Qiu, J.Y. Wang, W. Xi, High-performance flame retardancy by charcage hindering and free radical quenching effects in epoxy thermosets, Polymer 68 (2015) 262–269.
[17] Q. Lv, J.Q. Huang, M.J. Chen, J. Zhao, Y. Tan, L. Chen, Y.Z. Wang, An effective flame retardant and smoke suppression oligomer for epoxy resin, Ind. Eng. Chem. Res. 52 (27) (2013) 9397–9404.
[18] B. Schartel, A.I. Balabanovich, U. Braun, U. Knoll, J. Artner, M. Ciesielski, M. Döring, R. Perez, J.K.W. Sandler, V. Altstädt, T. Hoffmann, D. Pospiech, Pyrolysis of epoxy resins and fire behavior of epoxy resin composites flame-retarded with 9,10-dihydro-9-oxa-10-phosphaphenanthrene-10-oxide additives, J. Appl. Polym. Sci. 104 (4) (2007) 2260–2269.
[19] G. Beyer, Short communication: carbon nanotubes as flame retardants for polymers, Fire Mater. 26 (2002) 291–293.
[20] G. Beyer, Filler blend of carbon nanotubes and organoclays with improved char as a new flame retardant system for polymers and cable applications, Fire Mater. 29 (2005) 61–69.
[21] T. Kashiwagi, E. Grulke, J. Hilding, R. Harris, W. Awad, J. Douglas, Thermal degradation and flammability properties of poly(propylene)/carbon nanotube composites, Macromol. Rapid Commun. 23 (2002) 761–765.
[22] T. Kashiwagi, E. Grulke, J. Hilding, K. Groth, R. Harris, K. Butler, J. Shields, S. Kharchenko, J. Douglas, Thermal and flammability properties of polypropylene/carbon nanotube nanocomposites, Polymer 45 (2004) 4227–4239.
[23] B. Schartel, P. Pötschke, U. Knoll, M. Abdel-Goad, Fire behaviour of polyamide 6/multiwall carbon nanotube nanocomposites, Eur. Polym. J. 41 (2005) 1061–1070.
[24] T. Kashiwagi, F.M. Du, J.F. Douglas, K.I. Winey, R.H. Harris, J.R. Shields, Nanoparticle networks reduce the flammability of polymer nanocomposites, Nat. Mater. 4 (2005) 928–933.
[25] T. Kashiwagi, J. Fagan, J.F. Douglas, K. Yamamoto, A.N. Heckert, S.D. Leigh, J. Obrzut, F.M. Du, S. Lin-Gibson, M.F. Mu, K.I. Winey, R. Haggenmueller, Relationship between dispersion metric and properties of PMMA/SWNT nanocomposites, Polymer 48 (2007) 4855–4866.
[26] P.A. Song, L.H. Xu, Z.H. Guo, Y. Zhang, Z.P. Fang, Flame-retardant-wrapped carbon nanotubes for simultaneously improving the flame retardancy and mechanical properties of polypropylene, J. Mater. Chem. 18 (42) (2008) 5083–5091.
[27] H.Y. Ma, L.F. Tong, Z.B. Xu, Z.P. Fang, Functionalizing carbon nanotubes by grafting on intumescent flame retardant: nanocomposite synthesis, morphology, rheology, and flammability, Adv. Funct. Mater. 18 (2008) 414–421.
[28] H.O. Yu, J. Liu, X. Wen, Z.W. Jiang, Y.J. Wang, L. Wang, J. Zheng, S.Y. Fu, T. Tang, Charing polymer wrapped carbon nanotubes for simultaneously improving the flame retardancy and mechanical properties of epoxy resin, Polymer 52 (21) (2011) 4891–4898.
[29] K.Q. Zhou, J.J. Liu, Y.Q. Shi, S.H. Jiang, D. Wang, Y. Hu, Z. Gui, MoS_2 nanolayers grown on carbon nanotubes: an advanced reinforcement for epoxy composites, ACS Appl. Mater. Interfaces 7 (11) (2015) 6070–6081.
[30] D.Y. Wang, Y. Liu, Y.Z. Wang, C. Perdomo Artiles, T. Richard Hull, D. Price, Fire retardancy of a reactively extruded intumescent flame retardant polyethylene system enhanced by metal chelates, Polym. Degrad. Stabil. 92 (8) (2007) 1592–1598.
[31] X.Y. Wang, Y. Li, W.W. Liao, J. Gu, D. Li, A new intumescent flame-retardant: preparation, surface modification, and its application in polypropylene, Polym. Adv. Technol. 19 (8) (2008) 1055–1061.
[32] B. Schartel, T.R. Hull, Development of fire-retarded materials—Interpretation of cone calorimeter data, Fire Mater. 31 (2007) 327–354.
[33] J.Y. Wang, L.J. Qian, B. Xu, W. Xi, X.X. Liu, Synthesis and characterization of aluminum poly-hexamethylenephosphinate and its flame-retardant application in epoxy resin, Polym. Degrad. Stabil. 122 (2015) 8–17.
[34] S. Brehme, B. Schartel, J. Goebbels, O. Fischer, D. Pospiech, Y. Bykov, M. Döring, Phosphorus polyester versus aluminium phosphinate in poly(butylene terephthalate) (PBT): flame retardancy performance and mechanisms, Polym. Degrad. Stabil. 96 (2011) 875–884.
[35] A. König, E. Kroke, Flame retardancy working mechanism of methyl-DOPO and MPPP in flexible polyurethane foam, Fire Mater. 36 (2012) 1–15.